IN-SITU DAMAGE MONITORING AND CORRELATION WITH ACOUSTIC EMISSION IN CFRP COMPOSITES

Fatih E. Oz[1], Nuri Ersoy[2] and Stepan V. Lomov[3]

[1]Department of Mechanical Engineering, Bogazici University, Bebek, 34342, Istanbul, Turkey
Email: fatih.oz@boun.edu.tr, web page: http://www.composites.boun.edu.tr

[2]Department of Mechanical Engineering, Bogazici University, Bebek, 34342, Istanbul, Turkey
Email: nuri.ersoy@boun.edu.tr, web page: http://www.composites.boun.edu.tr

[3]Department of Materials Engineering, KU Leuven, Kasteelpark Arenberg 44, 3001 Leuven, Belgium
Email: stepan.lomov@kuleuven.be, web page: www.composites-kuleuven.be

Keywords: CFRP, Digital Image Correlation, Acoustic Emission, Damage Identification

ABSTRACT

The purpose of this study is to identify Acoustic Emission (AE) characteristics of damage modes in quasi-isotropic Carbon Fibre Reinforced Polymeric (CFRP) composites under quasi-static tension tests. $[-45_2/90_2/+45_2/0_2]_s$ - $[90_2/+45_2/0_2/-45_2]_s$ - $[0_2/-45_2/90_2/+45_2]_s$ laminates are considered in this study. AE is assumed to be a promising technique for damage detection in composite materials but it is only not sufficient to classify damage modes corresponding to AE events. An unsupervised k++ means clustering algorithm is applied to investigate the peculiarities of AE features. It is seen that cluster properties are different for each laminate type. In order to have a reliable correlation between damage modes and AE clusters, two in-situ optical observation instruments are used with AE technique during tension tests. First one is Digital Image Correlation (DIC). It is used for strain measurement and to see damage on surface of the specimens. Second one is in-situ observation of damage at interior plies from a 5 mm frame of free edge by a CCD camera with high magnification lens. Each optical method provides useful information where AE is insufficient to identify the damage modes. Optical methods prove that even though similar damage modes are induced in each laminate type, their AE correspondence is different. At the end of this study, reliable damage mode identification and classifications are obtained for quasi-isotropic CFRP laminates.

1 INTRODUCTION

Tension stress-strain responses of composite materials are almost linear curves and it is difficult to detect first ply failure level and damage progression from single tension test. Additional techniques are required to determine first damage level and damage accumulation. Acoustic Emission (AE) is assumed to be a promising technique for this manner. AE registration is a useful methodology, which allows "hearing" and identifying damage. An AE signal is an ultrasonic wave resulting from the sudden release of the strain energy when damage happens. When critical stress values are exceeded in a material, it fails locally (on microscale) and the strain energy stored is suddenly released where mechanical stress waves are induced. These waves can be detected with suitable sensors. The mechanical information picked up from the material is then converted into an electrical signal. Each of these signals contains information in time and frequency domain that are originated from a micromechanical event. Damage threshold levels can be detected easily with this method however damage mode identification is not so straightforward. There are lots of studies in literature using AE technique for damage mode identification in composite materials. Some of these studies classified damage modes with respect to single AE features. Amplitude and peak frequency are generally used for the classification. However, this method is contentious. Because, amplitude values of same damage mode can be affected with the distance between the sensors and location of damage. This is also true for peak frequency. In addition to this, sensor types can affect the peak frequency values of recorded AE events. Some other studies used clustering algorithms which enable multi-parametrical analysis of AE events. It evaluates features

of AE events collectively and provides a classification with respect to the relationship between AE features. Although this method can distinguish the AE events in a more reliable way, it is still not sufficient for a correct correlation between AE clusters and damage modes. Optical evidences are required for this manner.

The purpose of this study is to identify Acoustic Emission (AE) characteristics of damage modes in quasi-isotropic Carbon Fibre Reinforced Polymeric (CFRP) composites under quasi-static tension tests. Three different lay-ups are considered in this study: $[-45_2/90_2/+45_2/0_2]_s$ - $[90_2/+45_2/0_2/-45_2]_s$ - $[0_2/-45_2/90_2/+45_2]_s$. It is seen that characteristics of AE features are different for each laminate type. It is not possible to determine damage modes with respect to AE results directly. So, k++ means clustering algorithm, developed by Li et. al [1-3] is applied to investigate the peculiarities of AE features for each laminate type. It is seen that cluster properties are different for each laminate type. In order to have a correct and reliable correlation between damage modes and AE clusters, two in-situ optical observation instruments are used with AE technique during tension tests. First one is Digital Image Correlation (DIC). It is used for strain measurement and to visualize damage on the surface of specimens. Second one is in-situ observation of damage at interior plies from a 5 mm frame of free edge by a CCD camera with high magnification lens. Each optical method provides useful information where AE is insufficient to identify the damage modes. Optical methods prove that even though similar damage modes are induced in each laminate type, their AE correspondence. At the end of this study, reliable damage mode identification and classifications are obtained for quasi-isotropic CFRP laminates.

2 MATERIAL AND EXPERIMENTAL METHODOLOGY

Material used in this study is Hexcel's AS4/8552. Its fibre volume fraction and nominal thickness are 57.4 % and 0.184 mm respectively. A large plate with dimensions of 455 x 455 mm is manufactured in the autoclave at Bogazici University Composites Laboratory. Specimens are cut from this plate with a diamond saw in regarding directions to obtain $[-45_2/0_2/+45_2/90_2]_s$ - $[90_2/+45_2/0_2/-45_2]_s$ - $[0_2/-45_2/90_2/+45_2]_s$ - laminates with 3 mm thickness, 15 mm width and 175 mm length. Quasi-isotropic GFRP composites with 1.5 mm thickness and 50 mm length are used as end tabs. Their gage section ends are tapered to 20°-30° to prevent failure from grip sections.

Tension tests are performed with electro-mechanical Instron 4505 testing machine according to ASTM D3039 standard [4] with a test rate of 1 mm/min. Specimens are loaded up to 70%, 80% and 90% of their ultimate strength.

Vallen AMSY-5 AE system with two broadband Digital Wave B-1025 sensors (frequency range 25-1600 kHz) is used for real time AE registration during tension tests. AE sensors are fixed on the specimens by using C-clamps and they are placed 50 mm away from each other. Only the AE events having amplitudes higher than 45 dB are considered as damage. Also, damages between the two sensors and at least 5 mm away from each sensor are recorded. Before each test, pencil lead break is done to measure the wave speed and calibrate the real location of damage with AE detection. It is found that average wave speed is measured as 5000 mm/sec and there is around 1 mm discrepancy between the real location of damage and AE detection.

Unsupervised k++ means clustering algorithm, developed by Li et. al. [1-3] is used to classify AE events. This algorithm can be summarized as follow; Nine AE features are extracted from an AE event which contain information about the damage. These are: Amplitude (A), Duration (D), Rise Time (R), Energy (E), logarithmic value of Energy (log E), peak frequency (FMAX) and frequency centroid (FCOG), Weighted Frequency (WF) and Rise Amplitude (RA). In the first step of the algorithm, statistically representative features are selected with respect to Laplacian Score and Correlation Coefficient. AE features with higher score and less dependency to others are chosen for the next step, which is Principal Component Analysis (PCA). It is an orthogonal linear transformation that transforms multidimensional AE data into lower dimension set with a new coordinate system. Then optimal number of clusters is chosen with respect to two evaluation indices. First one is Silhouette Coefficient (SC). Higher SC score means dense and well-separated clusters. Second one is Davies-Bouldin (DB) index which is based on a ratio within-cluster and between-cluster distances and it relates to the cluster centroids. Combination of higher SC and lower DB index means better cluster quality. Finally, k-

means++ algorithm is used to generate clusters. It is based on an iterative algorithm where data samples are distributed to the closest centroids.

LIMESS system, with two CCD cameras, is used to acquire photos during tests. Photo acquisition is done with rate of 2 photos/second by VIC-Snap software. First camera is used for DIC calculations. A speckle pattern is painted on one surface of the specimen for this aim. Postprocessing of the photos enables to calculate the deformation during testing for full field strain maps by using the displacement of speckles on the surface. Obtained strain maps can also be used to detect damage on laminate surfaces. Second CCD camera has a high magnification lens used for in-situ observation of inner plies from a 5 mm frame on free edge of the specimen. It enables to identify micro damages at inner plies which are not possible to detect with DIC technique. The whole experimental setup used in this study can be seen in Figure 1.

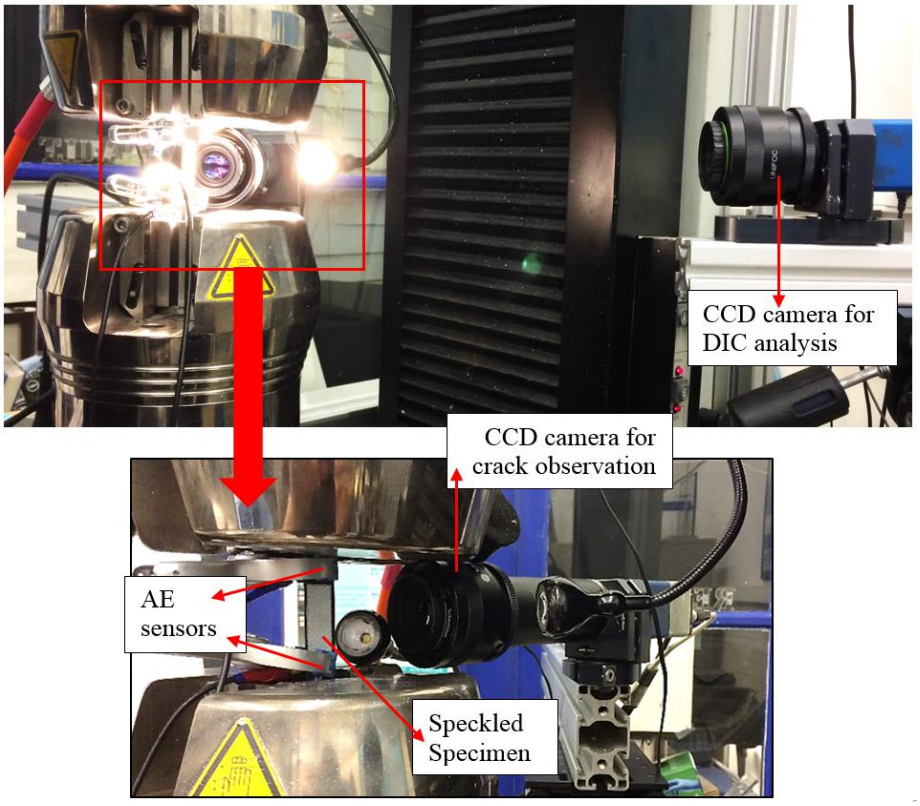

Figure 1. Experimental setup

3 RESULTS AND DISCUSSION

Tension test results with respect to cumulative AE energy and peak frequency values are presented in Figure 2. It shows that tests are highly repeatable and consistent. Damage initiation starts at very similar strain levels at each test. Average strain level for damage initiation is 0.48% for all laminate types. Figure 2 shows that while there are lots of high frequency events for $[-45_2/0_2/+45_2/90_2]_s$ and $[0_2/+45_2/90_2/-45_2]_s$ laminates, this is not the case for $[90_2/-45_2/0_2/+45_2]_s$ laminates. On the other hand, cumulative AE energy developments are highly different for each laminate. AE energy of first damage initiation is very high (Energy>1+E7) and then the cumulative AE energy curve reaches a plateau value for $[-45_2/0_2/+45_2/90_2]_s$. For $[90_2/-45_2/0_2/+45_2]_s$ laminate the energy level of first damage initiation is low (1+E4>Energy>1+E3), then it increase sharply which is an indication of sudden damage. Damage evolves continuously in $[0_2/+45_2/90_2/-45_2]_s$ laminates throughout the test.

Moreover, it was mentioned in previous studies that high frequency groups in AE results represent fibre breaks [1-3, 5-8]. This statement is contentious for the results in Figure 2. High frequency events are recorded during early strain levels for $[-45_2/0_2/+45_2/90_2]_s$ and they disappear after 0.70% strain. If

the previous statement is true, then it means that all the fibres are broken until 0.70% strain. This statement is not realistic since the laminate can still sustain load afterwards. Moreover for $[0_2/+45_2/90_2/-45_2]_s$ laminate, one cannot claim that fibres start and continue to fail from the first damage initiation level until the end of the test. One cannot give a . Results presented in Figure 2.a and 2.b are unexpected according to the assumption for fibre breaks in literature.

It is not possible to interpret and correlate AE results in Figure 2 with damage modes directly. AE clusters and damage evolution during loading are presented in further subsections for each laminate type.

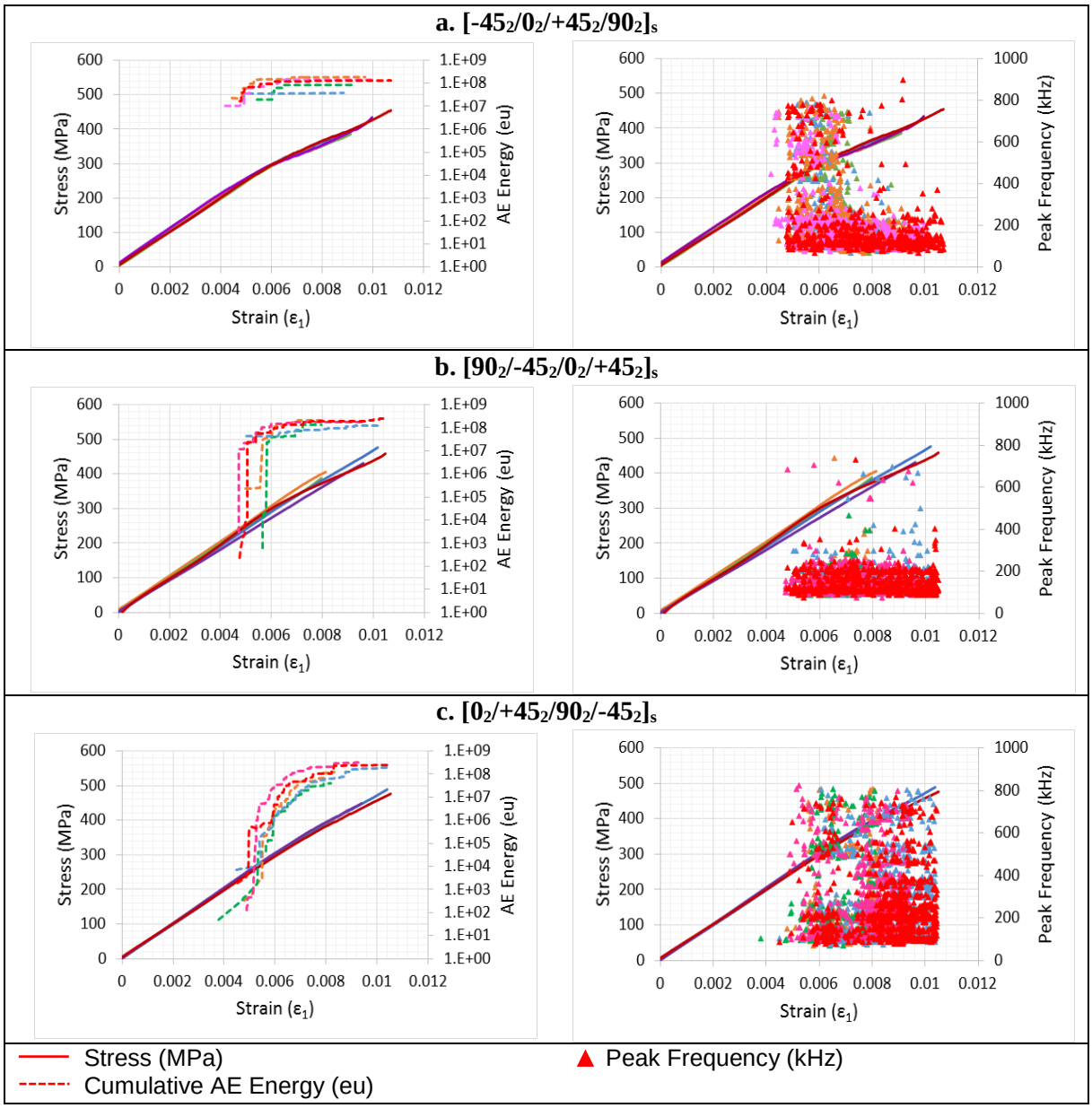

Figure 2. Stress-strain curves and AE registration for test laminates, data for five specimens are shown with different colours: (a) $[-45_2/0_2/+45_2/90_2]_s$ (b) $[90_2/-45_2/0_2/+45_2]_s$ (c) $[0_2/+45_2/90_2/-45_2]_s$

3.1 Cluster Groups

Peak frequency and cumulative AE energy curves in Figure 2 imply that there are peculiarities in clustering properties for each laminate. For instance, while most of the peak frequency values are between 0-300 kHz for $[90_2/-45_2/0_2/+45_2]_s$ laminate in Figure 2.b, there is large scatter for $[0_2/+45_2/90_2/-45_2]_s$ laminate between 0-800 kHz in Figure 2.c. It is found that peak frequency is a statistically representative feature for $[0_2/+45_2/90_2/-45_2]_s$ but not for $[90_2/-45_2/0_2/+45_2]_s$ laminate according to the clustering algorithm. Clusters are well seperated with respect to weighted frequency (WF) and amplitude (A) values. Cluster groups for each laminate is shown in Figure 3. Details of clustering are not presented here for the sake of brevity.

Figure 3 shows that cluster groups are highly different for each laminate. It should be mentioned that the only difference between laminates is their lay-up orientation in Figure 2 and Figure 3. Similar damage modes are expected to occur within them. AE characteristics of similar damage modes are different in each laminate type. That's why clusters in Figure 3 are generated differently by the algorithm. Cluster boundaries are not emphasized here as in previous studies [1-3,9]. Accumulation AE events of the clusters throughout the test is presented and discussed in the next subsection.

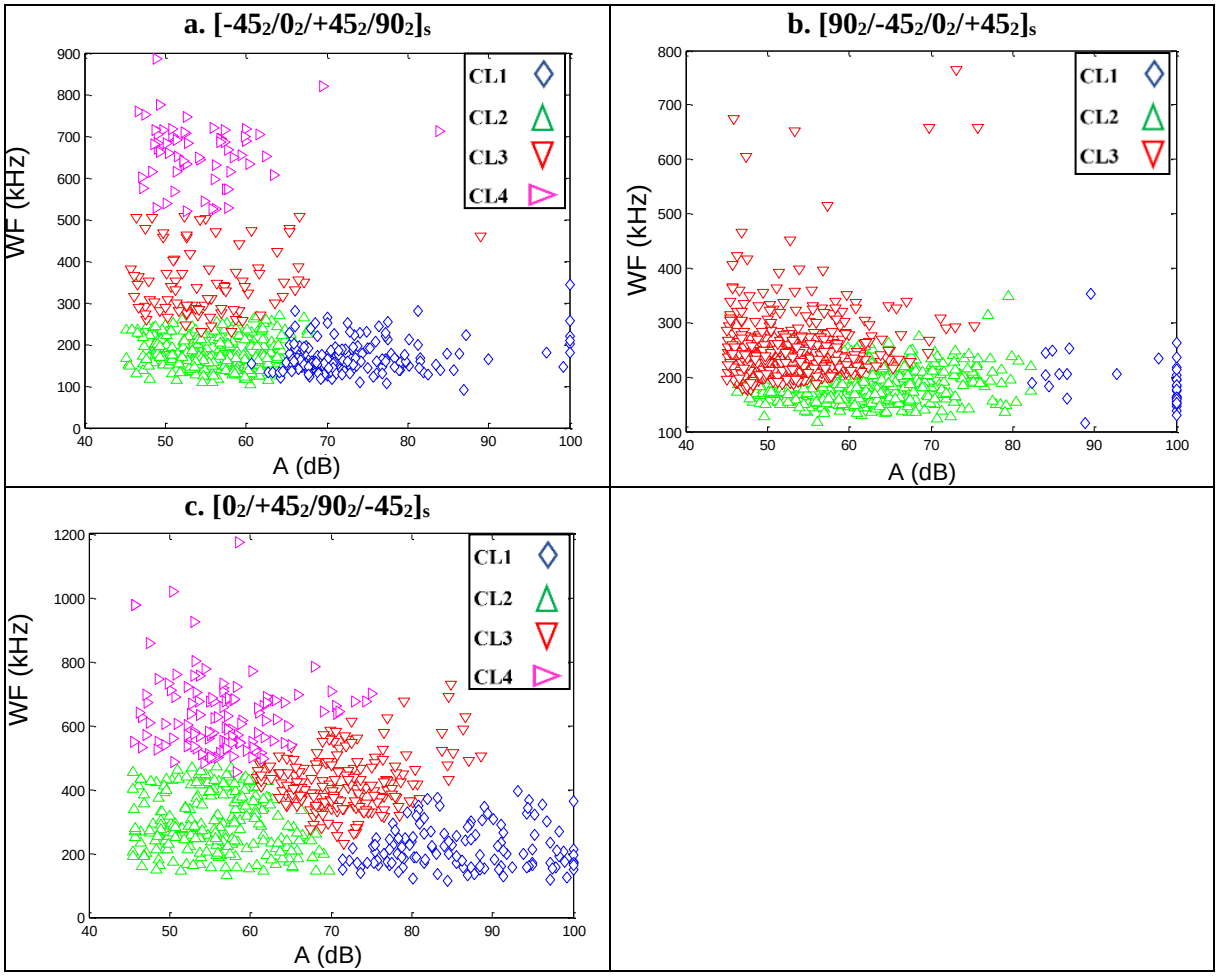

Figure 3. Seperation of cluster groups for (a) $[-45_2/0_2/+45_2/90_2]_s$ (b) $[90_2/-45_2/0_2/+45_2]_s$ (c) $[0_2/+45_2/90_2/-45_2]_s$

3.2 Damage Mode Correlation

In this subsection, each laminate type is discussed separately to correlate the AE characteristics to the monitored damage modes. First one is $[-45_2/0_2/+45_2/90_2]_s$. Accumulation of clusters throughout the test can be seen in Figure 4. Clusters with high frequency and low amplitude features (CL3-CL4) are recorded until around 0.70% strain where high amplitude and low frequency cluster (CL1) is seen after 0.70% strain levels. They are obviously different damage groups. According to assertions in literature, CL3 and CL4 should be fibre breaks due to their high frequency characteristics [1-3, 5-8]. But they occur before 0.70% strain and dissapear afterwards and it makes previous statement doubtful. It is not easy to identify them without optical observations.

Figure 5 presents damage evolution throughout the test. Very left column of Figure 5 shows the strain levels of test which is the average of ε_1 strain calculated with DIC. Captures of micro damage evolution from 5 mm edge frame can be seen on the second column of Figure 5. 5 mm frame of the edge that is observed by optical microscope and its distance to AE sensor are marked on Figure 5. Purple color represents the lowest values for ε_1 and ε_2 strain maps and increases are shown with shades of blue, green, yellow and red respectively. Damage development throughout the test is as follow; first damage is observed at 0.58% strain by edge observation in Figure 5. It is transverse matrix crack in mid-90° plies. Then it propagates to adjacent lower 45° plies. At the same time, there is micro delamination at 90°/45° interface. Similar damage mode induces 3 mm away from the first damage at 0.70% strain. DIC strain map for ε_2 shows that at 0.70% strain, there is very high contraction on one side of the specimen. That is due to seperation of 90° and 45° plies, which is named as macro delamination in this paper. Similar damage mode initiates from the observed side of the specimen at 0.80% strain level and propagates through the gauge length. The seperation of 90° and 45° plies from each other can be seen from the edge camera when the strain of the test is 0.87% as shown in Figure 5. It is worth noting that this delamination can be detected with 2D DIC technique. This is an important result obtained in this study.

Correlation of damage modes and AE clusters can be done with in-situ optical observations. Before 0.70% strain, only micro cracks at inner plies are observed. Most of the recorded events before 0.70% strain belong to clusters CL3 and CL4. At around the strain level of 0.70% the propagation of macro delamination is completed through the gauge length near one side of the laminate. Separation of layers still continue through gauge length and width, and at the same time density of high amplitude-low frequency cluster (CL1) increases considerably. So CL3-CL4 clusters can be classified as transverse matrix cracks in 90° and 45° plies. CL1 can be classified as the macro delamination with AE characteristics are high amplitude with low frequency. CL2, with low amplitude and low frequency properties, corresponds to the micro delaminations between the layers. So high frequency clusters (CL3-CL4) are not fibre breaks, which is proven by optical evidences.

Second laminate presented in Figure 2.b is $[90_2/-45_2/0_2/+45_2]_s$. In this laminate, all peak frequency values are lower than 300 kHz. It means that frequency parameters are not statistically representative features. It can also be noticed in Figure 3.b that weighted frequency distribution is very similar for all amplitudes. Figure 6 shows the accumulation of clusters throughout the test. Figure 7 shows that surface damage can be clearly identified with DIC as surface cracks at 0.65% strain. A micro crack initiates at bottom surface of the laminate. At the same time it causes adjacent -45° ply to crack with a delamination between them. At 0.76% strain a correlation between DIC strain maps and edge observation can be done. The crack on top surface is captured with DIC maps and edge camera. Its distance to AE sensor is measured to be 21.5 mm. Amplitude of this damage has the highest value (100 db) at 0.76% strain in Figure 6. Meanwhile, there are multiple AE events recorded just after it, with lower amplitudes. Although there seems to be some other events recorded at different regions, these events are not verified by optical observations and thought to be reflections of the waves propagated from the first damage. As mentioned before, surface cracks cause damage in adjacent -45° plies and delamination between 90°/-45° interface immediately through the width of the laminate. So it is not possible to match a single crack with a particular AE event, since cracks can cause some wave reflections within the laminate. One correlation that can be positively asserted is, high amplitude cluster in Figure 6 (CL1) correspond the surface cracks for $[90_2/-45_2/0_2/+45_2]_s$ laminate.

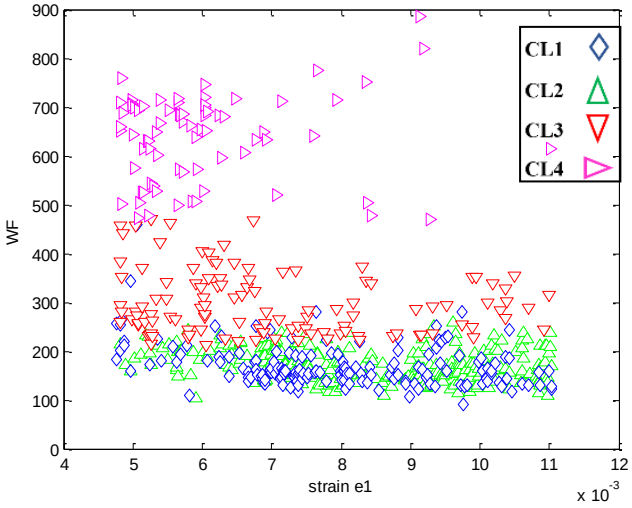

Figure 4. Accumulation of AE clusters throughout a test in $[-45_2/0_2/+45_2/90_2]_s$ laminate

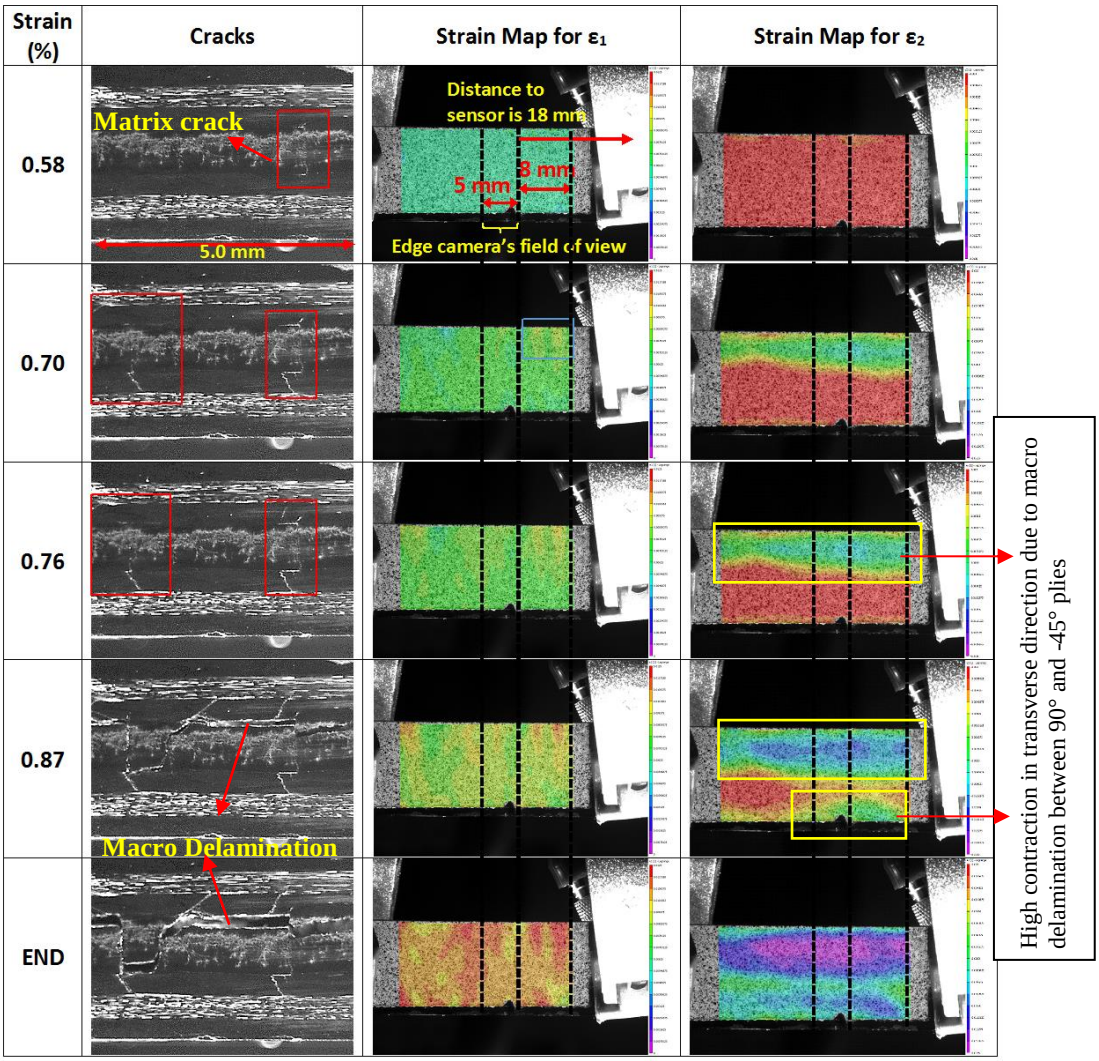

Figure 5. Damage accumulation in $[-45_2/0_2/+45_2/90_2]_s$ laminate

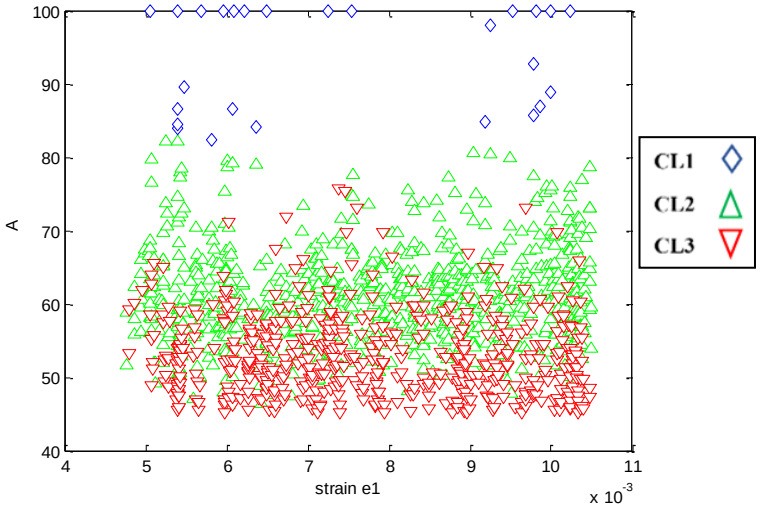

Figure 6. Accumulation of AE clusters throughout the test in $[90_2/-45_2/0_2/+45_2]$s laminate.

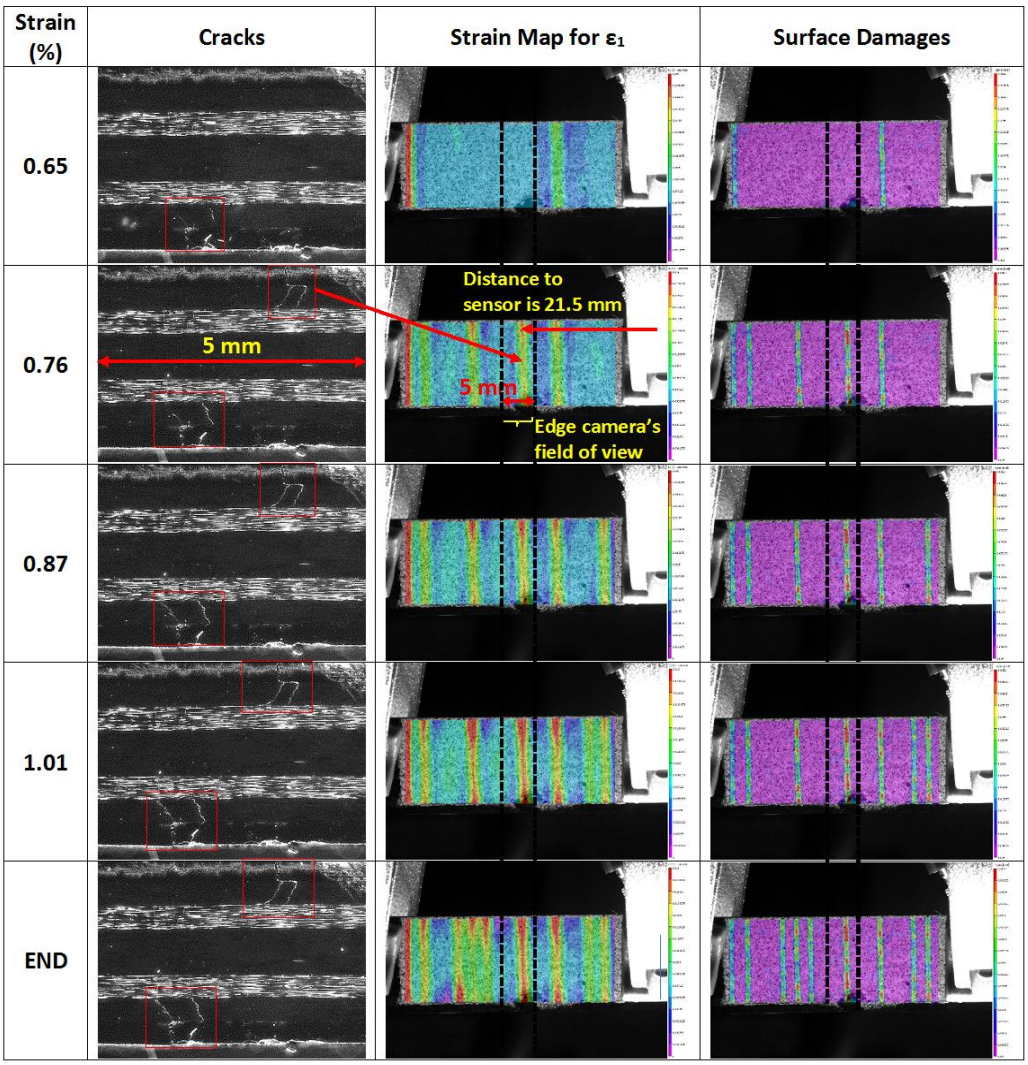

Figure 7. Damage accumulation in $[90_2/-45_2/0_2/+45_2]_s$ laminate

Third laminate in consideration is $[0_2/+45_2/90_2/-45_2]_s$. As shown on Figure 2.c, amount of high frequency events is very high. Frequency parameters are highly selective for this laminate type. Accumulation of AE clusters throughout the test with respect to WF and damage progression are shown in Figure 8. Density of each cluster except CL3 increase after 0.60% strain. Density of CL3 increases after 0.80% strain as seen in Figure 8.a.

Figure 8.b presents micro damage evolution throughout the test. Strain maps obtained by DIC do not provide useful information about damage mode identification, so they are not presented for this laminate. Figure 8.b shows that there is a high number of transverse cracks in 90° plies until the end of the test. First damage occurs at 0.63% strain. As in previous laminates, induced damage is not a single mode. Transverse crack in 90° ply occurs with micro delaminations between adjacent -45° and +45° plies. Until 0.83% strain, only transverse cracks in 90° plies with micro delaminations between -45°/90° and +45/90 interfaces are observed. After this strain level, damage in mid -45° ply can be seen from the edge of the specimen in Figure 8.b. Propagation of this damage through the thickness of mid -45° ply is completed at 0.88% strain. Damage in mid -45° ply initiates from inner section of the laminate, propagates through the width and then through the thickness of the laminate as seen in Figure 8.b. It is consistent with accumulation of CL3 in Figure 8.a. High amount of accumulation of CL3 at 0.80% strain in Figure 8.a means that damage in mid -45° plies initiates at 0.80% strain at inner parts. Its propagation to the monitored edge frame is completed at 0.83% strain and propagation through the thickness of mid -45° ply is completed right after at 0.88% strain. So, it is obvious that CL3 in Figure 8.a represents AE characteristics of transverse cracks in mid -45° plies.

As mentioned before, first damage mode observed is transverse cracks in 90° plies with delaminations between adjacent -45° and +45° plies. In order to correlate these damage modes with AE features, accumulation of cracks observed at the edge frame until the end of the test is compared with number of events from clusters in recorded in the same frame. Figure 9 shows that the number of transverse cracks is highly consistent with CL1 and CL4. Former is a cluster with high amplitude events whereas the latter consist of lower amplitude but high frequency events. It is highly possible that high frequency cluster belongs to transverse cracks at 90° plies since it is located at inner section as in $[-45_2/0_2/+45_2/90_2]_s$ laminate and CL1 is delamination at -45/90 and +45/90 interfaces. Although deeper investigation is required to discriminate the correspondence of these clusters, still a satisfactory correlation is obtained between AE characteristics and damage modes that occur simultaneously; namely transverse cracks in 90° plies and delamination between -45/90 and+45/90 py interface.

It is seen from the laminates considered in this study that; transverse cracks in 90° and ±45° plies correspond to high frequency-low amplitude clusters in $[-45_2/0_2/+45_2/90_2]_s$ and $[0_2/+45_2/90_2/-45_2]_s$ laminates whereas it corresponds to high amplitude cluster in $[90_2/-45_2/0_2/+45_2]_s$ laminate. The location of 90° plies have an imporant effect on AE characteristics of transverse matrix cracking.

4 CONCLUSIONS

In this study, k-means++ clustering algorithm is used to classify AE events. AE registration itself cannot be sufficient to identify all damage modes. In-situ optical observations enable to make reliable correlations between AE clusters and damage modes.

It is observed that, lay-up orientations have a considerable effect on AE characteristics of damage modes. The first damage mode observed is transverse matrix cracks in 90° plies in all laminates and the AE characteristics of this damage mode is different in each laminate type. If 90° plies are the inner plies, the AE characteristics is high frequency and low amplitude events, whereas if 90° plies are surface plies, then its AE characteristics are high amplitude and low frequency events. This study proves that high frequency events do not correspond to fibre breakage as assumed in the literature. It is found that they are generally transverse matrix cracks at inner 90° plies. Also, 2D DIC technique can detect delamination of layers through the thickness, which is named as macro delamination.

These aforementioned damage modes would not have been identified if in-situ optical observation instruments were not used.

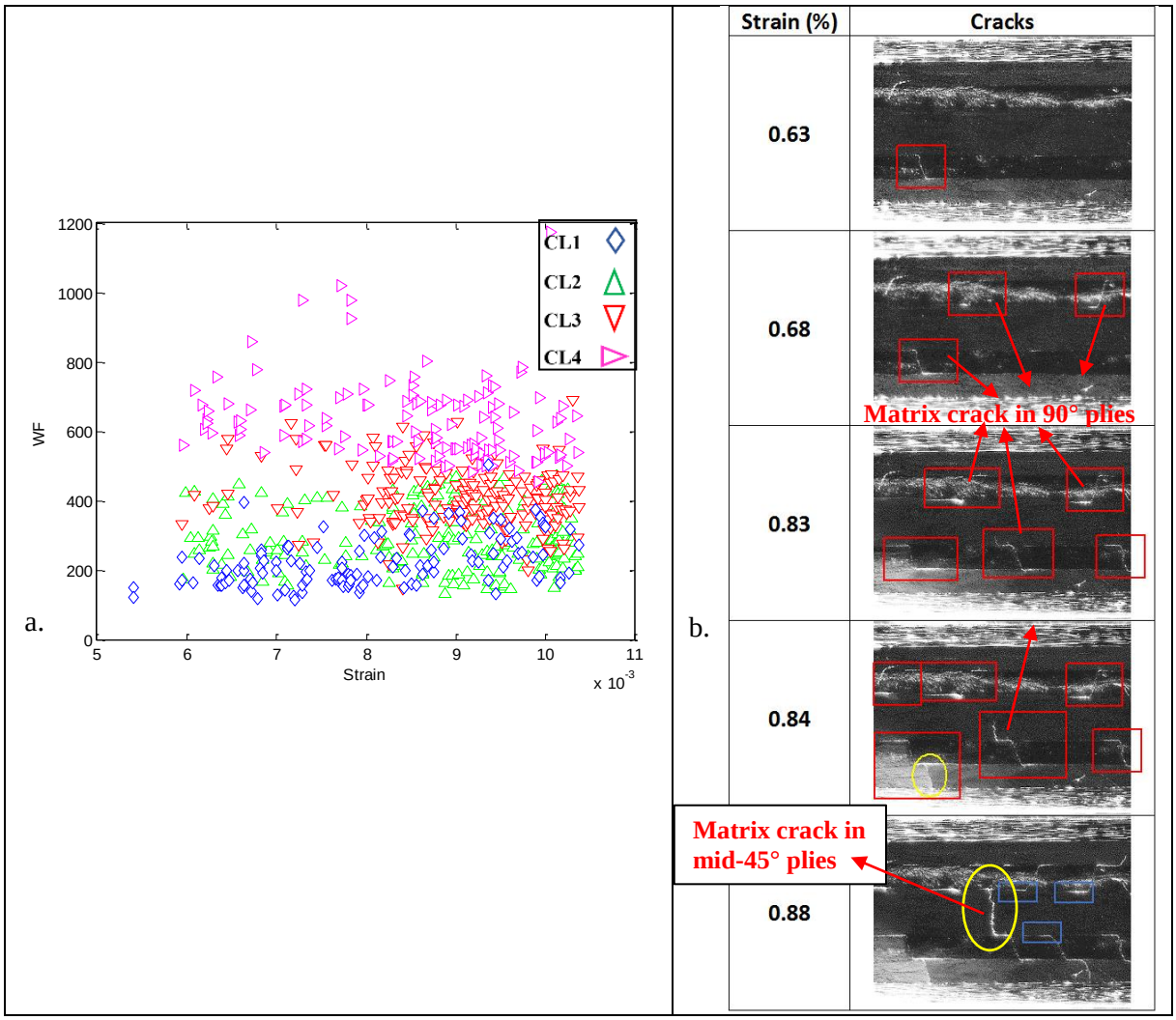

Figure 8. a: Accumulation of AE clusters throughout a test in $[0_2/+45_2/90_2/-45_2]_s$ laminate, b: Damage accumulation in $[0_2/+45_2/90_2/-45_2]_s$ laminate

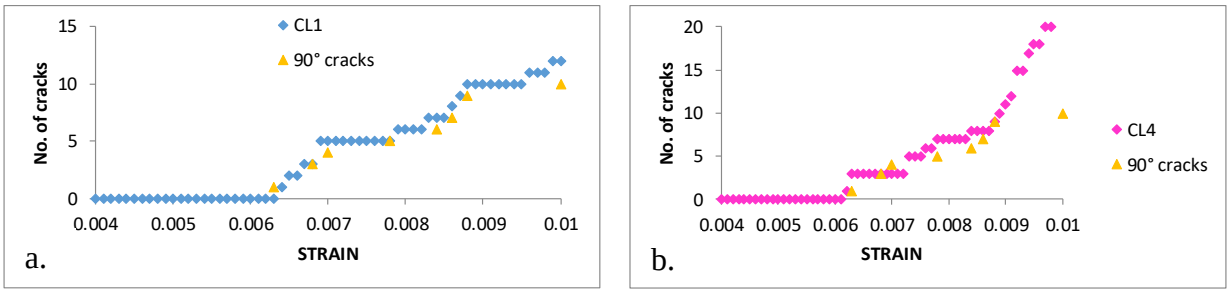

Figure 9. a: Comparison of clusters with number of cracks with high amplitude cluster, b: lower amplitude but high frequency cluster

ACKNOWLEDGEMENTS

Authors acknowledge the support of the Boğaziçi University Research Fund, Istanbul Development Agency (ISTKA) and TUBITAK BIDEB-2214/A under project codes 10020/15A06D3, ISTKA/BIL/2012/58 and 1059B141600673 respectively.

REFERENCES

[1] L. Li, S.V. Lomov, X. Yan, V. Carvelli, Cluster analysis of acoustic emission signals for 2D and 3D woven glass/epoxy composites. *Composite Structures*, **116 (1)**, 2014, pp. 286-299 (https://doi.org/10.1016/j.compstruct.2014.05.023).

[2] L Li, Y Swolfs, I Straumit, X Yan, S.V. Lomov, Cluster analysis of acoustic emission signals for 2D and 3D woven carbon fiber/epoxy composites. *Journal of Composite Materials*, **50 (14)**, 2015, pp. 1921-1935 (https://doi.org/10.1177/0021998315597742).

[3] L Li, S.V. Lomov, X. Yan, Correlation of acoustic emission with optically observed damage in a glass/epoxy woven laminate under tensile loading. *Composite Structures*, **123**, 2015, pp. 45-53 (https://doi.org/10.1016/j.compstruct.2014.12.029.

[4] ASTM D3039/D3039M-14 Standard Test Method for Tensile Properties of Polymer Matrix Composite Materials, *ASTM International*, (https://doi.org/10.1520/D3039_D3039M-14).

[5] P.J. de Groot, P.A.M Wijnen, R.B.F Janssen, Real-time frequency determination of acoustic emission for different fracture mechanisms in carbon/epoxy composites. *Composites Science and Technology*, **55 (4)**, 1995, pp. 405-412 (https://doi.org/10.1016/0266-3538(95)00121-2).

[6] C.R. Ramirez-Jimenez, N. Papadakis, N. Reynolds, T.H Gan, P. Purnell, M. Pharaoh, Identification of failure modes in glass/polypropylene composites by means of the primary frequency content of the acoustic emission event. *Composites Science and Technology*, **64 (12)**, 2004, pp. 1819-1827 (https://doi.org/10.1016/j.compscitech.2004.01.008).

[7] R. Gutkin R, C.J. Green, S. Vangrattanachai, S.T Pinho, P. Robinson, P.T. Curtis, On acoustic emission for failure investigation in CFRP: Pattern recognition and peak frequency analyses. Mechanical Systems and Signal Processing, **25 (4)**, 2011, pp. 1393-1407, (https://doi.org/10.1016/j.ymssp.2010.11.014).

[8] R. Mohammadi R, M.A Najafabadi, M. Saeedifar, J. Yousefi, G. Minak, Correlation of acoustic emission with finite element predicted damages in open-hole tensile laminated composites. *Composites Part B: Engineering*, **108**, 2017, pp. 427-43, (https://doi.org/10.1016/j.compositesb.2016.09.101).

[9] V. Carvelli, A. D'Ettorre, S.V. Lomov, Acoustic emission and damage mode correlation in textile reinforced PPS composites, *Composite Structures*, **163**, 2017, pp. 399-409, (https://doi.org/10.1016/j.compstruct.2016.12.012).